Osmotic Pressure in a Bacterial Swarm

Osmotic pressure in a bacterial swarm

Liyan Ping[a], Yilin Wu[b], Basarab G. Hosu[a,c], Jay X. Tang[a,d], and Howard C. Berg[a,c,*]

[a]Rowland Institute at Harvard, Cambridge, Massachusetts

[b]Department of Physics, Chinese University of Hong Kong, Shatin, NT, Hong Kong, P. R. China

[c]Department of Molecular and Cellular Biology, Harvard University, Cambridge, Massachusetts

[d]Physics Department, Brown University, Providence, Massachusetts

Runing Title: Swarm Osmolarity

*Correspondence: hberg@mcb.harvard.edu.

Keywords: *Escherichia coli*, bacterial motility, liposome sensor

ABSTRACT Using *Escherichia coli* as a model organism, we have studied how water is recruited by a bacterial swarm. Previous analysis of trajectories of small air bubbles revealed a stream of fluid flowing in a clockwise sense ahead of the swarm. A companion study suggested that water moves out of the agar into the swarm in a narrow region centered ~30 μm from the leading edge of the swarm and then back into the agar (at a smaller rate) in a region centered ~120 μm back from the leading edge. Presumably, these flows are driven by changes in osmolarity. Here, we utilized green/red fluorescent liposomes as reporters of osmolarity in order to verify this hypothesis. The stream of fluid that flows in front of the swarm contains osmolytes. Two distinct regions are observed inside the swarm near its leading edge: an outer high-osmolarity band ~30 mOsm higher than the agar baseline and an inner low-osmolarity band isotonic or slightly hypotonic to the agar baseline. This profile supports the fluid-flow model derived from the drift of air bubbles and provides new insights into water maintenance in bacterial swarms. High osmotic pressure at the leading edge of the swarm extracts water from the underlying agar and promotes motility. The osmolyte is of high molecular weight, probably lipopolysaccharide.

INTRODUCTION

When some bacteria grow in a rich medium on the surface of moist agar, cells elongate, multinucleate, grow flagella, and swarm across the surface in coordinated packs (1-3). Swarming promotes invasiveness of bacterial pathogens, as has been confirmed in a wide range of clinical isolates, including *Pseudomonas aeruginosa*, *Proteus mirabilis*, *Bacillus cereus*, *Salmonella enterica*, *etc.*(4-7). In 1994, Harshey and Matsuyama discovered that strains of *Escherichia coli* K-12 swarm on Eiken agar (from Japan) rather than on Difco agar, presumably because Eiken agar is more wettable (8). Many bacteria produce surfactants as they swarm, which influences patterns of expansion (2, 3). However, these surfactants are not essential; in particular, there is no indication that *E. coli* produces surfactants (9). Absence of surfactants simplifies efforts to establish the role played in swarm expansion by osmotic flow.

An *E. coli* swarm consists of an actively expanding rim of cells followed by a relatively inactive interior (10, 11). The cells swim in a thin film of fluid, the upper surface of which is stationary (12). This film extends some 10-20 μm ahead of the leading edge of the swarm. Tracking of microbubbles prepared from the surfactant Span 83 indicated that this region of fluid streams clockwise in front of the swarm at a rate about 3 times that of the swarm advance (12). This chiral flow is driven by the counterclockwise rotation of the flagella of cells stalled at the edge of the swarm (12, 13). Patterns of flow of fluid within the swarm also were inferred from the motion of microbubbles. The data could be fit by a model in which a large amount of fluid moved from the agar into the swarm near its leading edge, while a smaller amount moved from the swarm back into the agar ~100 μm further behind (10). The bulk fluid in a swarm provides

the environment for flagellar rotation and for transportation of nutrients and signaling molecules. The only source for this fluid is the underlying agar. One of the intriguing questions is how water is extracted from the agar. Presumably, this occurs because the osmolarity of the fluid within the swam is higher than that within the agar.

In this work, we probed the change in osmolarity within *E. coli* swarms with osmolarity-sensitive liposomes, inspired by the work of Jayaraman *et al.*(14); see below. First we deposited liposomes in spots ~450 μm in diameter and collected fluorescence signals from entire spots as swarms ran over them. To improve the spatial resolution, we made liposome pads that were 5 times larger in diameter than the spots, allowed the swarms to run over them, and then scanned the pads with an excitation beam only 20 μm in diameter. We found that the osmolarity rises abruptly near the leading edge of the swarm, then drops to a level close to that of the virgin agar ~100 μm behind. The intervening region is one of high cell density. Evidently, growth in this region generates a substantial concentration of soluble osmolytes, which draw fluid out of the underlying agar. As the swarm expands, some of these osmolytes diffuse into the agar, raising its osmolarity above the initial value. Cells following behind the band of high cell density move over the region formerly covered by these cells and experience an osmolarily inversion that draws some fluid back into the agar. Thus, one expects to see the biphasic flow profile predicted by the fluid flow measurements. The excess fluid that remains in the swarm fuels its spreading.

MATERIALS AND METHODS

Swarm plates

Swarm agar contained 1% Bacto peptone, 0.3% beef extract, and 0.5 % NaCl (the swarm medium) and 0.48 % Eiken agar. For tests of the influence of plate osmolarity on swarming

70 velocity, 0.5 – 0.55% NaCl and 0.48– 0.55% Eiken agar were used. The agar was autoclaved or
71 melted in a microwave oven and cooled to ~60°C, and then 0.5% filter-sterilized arabinose was
72 added. 25 ml aliquots were pipetted into into 150 mm dia. × 15 mm deep Petri plates. The
73 plates were swirled gently to spread the agar over the entire plate, cooled for 15 min inside a
74 Plexiglas box, and then inoculated.

75 **Cell growth**

76 Bacterial strains AW405 (15) and HCB1668 (16) were grown under conditions described
77 previously (10). Both strains were used for preliminary work, and AW405 for the final
78 experiments. In brief, single bacterial colonies were cultivated in LB broth overnight at 30°C
79 and diluted 10^{-5} with swarm medium. 1 µl of this suspension was dispensed ~ 3 cm from the
80 edge of a swarm plate, and the plate was dried in the Plexiglas box for another 30 min, until the
81 inoculum was completely absorbed. Plates were incubated at 30°C and ~100% relative humidity.

82 **Liposome preparation**

83 Lipids (in chloroform) were purchased from Avanti Polar Lipids, Inc. The liposomes were
84 prepared from 20 mg L-α-phosphatidylethanolamine (from *E. coli*), 6 mg 1,2-dioleoyl-sn-
85 glycero-3-phosphoethanolamine-N-[methoxy(polyethylene glycol)-2000], 6 mg 1,2-dipalmitoyl-
86 sn-glycero-3-phosphoethanolamine-*N*-[methoxy(polyethylene glycol)-5000], and 3 mg
87 cholesterol (molar ratio of 1 : 0.04: 0.04 : 0.3). The mixture was dried with gently flowing
88 nitrogen gas in a rotating 50-ml round-bottom flask for 30 min followed by vacuum evaporation
89 for 3 h. The lipid film was hydrated with 1 ml dye solution under argon with agitation at 160 rpm
90 at room temperature for 2 h. 18.67 mg calcein (Life Technologies Corp.) and 1.21 mg
91 sulforhodamine-101 (Life Technologies Corp.) were dissolved in Buffer I that contained 0.27

92 mM KCl, 0.147 mM KH_2PO_4, 1.5 mM Na_2HPO_4, 0.2 mM Tris, 102 mM NaOH, and 5 mM NaCl.
93 The final pH was adjusted to 7.4 with 1 M HCl, and the osmolarity to 240 mOsm with 1 M NaCl.
94 Osmolarity was measured with an Osmette II osmometer (Precision Systems, Inc., Natick, MA).
95 0.5-ml aliquots of the multilamellar lipid vesicles generated by this procedure were stored in
96 argon at –20°C, where they were stable for a few months; typically, we used them within one
97 month.

98 The dye-encapsulated multilamellar vesicles were converted to unilamellar vesicles by 5
99 cycles of freezing in dry ice for 5 min and thawing at 50°C for 15 min. The unilamenllar vesicles
100 were then passed through a 0.8-μm Nuclepore Track-Etch membrane (Whatman) 21 times at
101 50°C with a Mini-Extruder (Avanti Polar Lipids, Inc.) that was preconditioned with Buffer I at
102 50°C for 20 min. This generates liposomes ~0.5 μm in diameter. The liposomes were cooled to
103 room temperature for 5 min before loading on a Sephadex G-50 coarse gel filtration column to
104 remove free dyes. To prepare the column, the Sephadex beads were swelled with Buffer II at 4°C
105 for 2 days. Buffer II differs from Buffer I in that it contained an additional 0.5 mM $CaCl_2$ and 0.5
106 mM $MgCl_2$. The Sephadex slurry loaded on a column (1 cm × 25 cm) was washed with 4
107 volumes of swarm medium. The liposomes were eluted with the same medium (osmolarity 245
108 mOsm), and collected in glass vials. The liposomes were stable for up to a week when stored at
109 4°C under argon; typically, we used them within 3 days. About 0.5 ml liposome suspension
110 could be generated in one preparation. Aliquots were stored in 8 vials. Each vial was used no
111 more than 3 times; otherwise, a new G/R ratio osmolarity calibration was performed. The
112 liposomes were quite hardy. They did not fuse on colliding with one another. Nor did they
113 break when pipetted onto the surface of agar or when struck by swimming cells. Had they done
114 so, the dyes would have diffused into the underlying agar.

115 **Fluorescence detection and imaging**

116 The swarm plates were mounted on the temperature-controlled stage of an upright microscope
117 (Nikon Optiphot2) as described in (10), except that a 20x bright-phase objective was used. The
118 entire setup, except for the photomultiplier power supplies and computer, was enclosed by a
119 black foamboard box. Fluorescence was excited by a cold white LED (Thorlabs) via an FITC/
120 Texas red fluorescence cube (Chroma). The fluorescence from calcein (G) and sulforhodamine-
121 101 (R) was detected by photon-counting photomultipliers (Hamamatsu H7421) connected to a
122 data-acquisition board (National Instruments USB6211), and quantified with custom software
123 written in LabView (National Instruments), which provided the G/R ratio.

124 10 nL liposome suspension was dispensed with a 0.5-µl Neuros syringe (Hamilton Co.,
125 Reno, NV) and formed a spot ~450 µm in diameter similar to the size of the microscope's field
126 of excitation. Liposome spots were placed at locations ahead of the swarm according to the
127 estimated swarm expansion rate, so that the bacteria would arrive 1.5 h later. Data acquisition
128 was started 30 min after dispensing. The liposomes ended up on the top of the agar and were
129 overrun by the advancing swarm.

130 Phase-contrast videos were recorded using a Hi-res Exvision CCD camera connected to a
131 digital video cassette recorder before and after recording the fluorescence signal, as described in
132 (10). Swarming speed was determined after importing the images to a computer, as described
133 before (10). Times on the traces were then converted to distance from the swarm edge using the
134 swarm expansion rate. To monitor the bacterial behavior on the liposome spots, continuous video
135 clips were recorded at the proximal edge, the distal edge, and in the middle of the spots.

Alternatively, snapshots of a few seconds were taken during a fluorescence recording session by transiently blocking the light path to the photomultipliers and activating the video system.

Scanning swarms moving on liposome pads

All scanning experiments were performed with standard swarm plates and a 40x bright-phase objective. 50 nl liposome suspensions were dispensed with the Neuros syringe to form liposome pads that were ~2.3 mm in diameter. The liposome pads were placed at locations where a swarm would arrive in ~2 h, based on the swarm expansion rate. The liposome pads had a thick edge ~100 μm wide. Only fluorescence signals from uniformly-distributed liposomes found within this edge were collected. The microscopic field of excitation was reduced to a diameter of 20 μm by closing the excitation beam field iris.

The observation field for phase contrast (~500 μm in diameter) was centered ~100 μm away from the proximal edge of the liposome pad, between the pad and the advancing swarm. The swarm movement was monitored with the Hi-res Exvision CCD camera, using the microscope tungsten source. When the bacteria reached the liposome pad, the light path was switched to the photomultipliers and fluorecence signals were recorded. After 10-40 s, the swarm plate was pushed by an Intelligent Picomotor (New Focus, San Jose, CA) at 10, 20, or 30 μm/s, so that the excitation beam scanned the swarm in the swarm's direction of motion. Scanning was continued until the excitation beam reached the far edge of the pad, and then the plate was quickly pulled back manually and a 2nd scan initiated. The location of the interface between the monolayer and multilayer region of the swarm – see Fig.1 of (10) – was determined by briefly looking through the microscope during the scanning process. The swarming speed on agar was determined from the phase contrast video taken before the fluorescence scanning. The

158 swarming speed on liposome spots or pads was based on videos taken on swarms that were not
159 subjected to fluorescence recording. The traces of G/R ratios of the two scans were
160 superimposed after determining distances from the monolayer/multilayer interface, which was
161 taken as position 0.

162 **Calibration curves**

163 To convert the G/R ratio to osmolarity, we plotted two kinds of standard curves (Fig. 1). The
164 G/R ratio in solutions of different osmolarities was determined by mixing 1 μl liposome
165 suspension with 44 μl standard swarm medium or standard solution in a silicon-grease well on a
166 microscopic slide. Two 0.46 mm spacers made from double-sided Scotch tape and the paper
167 disks supplied with Millipore filters were placed outside the grease ring to fix its depth, and a
168 narrow channel was included through its wall to relieve the pressure when a coverslip was added
169 to seal the top. This channel was sealed with grease before the measurements were made.
170 Standard swarm media were prepared by adding different amounts of NaCl to swarm media, and
171 their osmolarities were measured with the Osmette II osmometer. Standard solutions were either
172 purchased from Precision Systems Inc., or made by adding 1 M NaCl to Buffer I. The slide was
173 prewarmed for 5 min at 30°C in the dark, and the fluorescence signal was recorded for 500 s at
174 30°C. The averaged values of G/R ratios obtained between 300 s and 350 s were used to plot the
175 calibration curves. The part after 250 s was fitted by linear regression to determine the photo-
176 bleaching rate.

177 Swarm plates with different osmolarity were prepared by adding different amounts of NaCl
178 to the swarm agar. A 10 nL liposome suspension was dispensed on the agar plate. After 30 min
179 incubation in the dark, fluorescence signals were recorded for 2 h. Then 0.5 mL agar was

scratched from the plate and centrifuged at 16,000 g for 20 min. 50 ul clean supernatant was taken out for determination of the osmolarity with the Osmette II osmometer. The G/R traces were then fitted by linear regression, and corrected for photo-bleaching. The curves corrected for photo-bleaching were extrapolated back 30 min to obtain the values for the G/R ratios free of the influence of evaporation. These values were used to plot the standard curves for liposomes on an agar surface. The calibration curves of the scanning experiments were obtained with a procedure similar to the real experiment, but on control plates with different osmolarities. The liposome pads were equilibrated 30 min before scanning, so that dense packing of liposomes would not occur.

RESULTS AND DISCUSSION

Osmolarity-sensitive liposomes

Liposomes were prepared by a recipe adapted from Jayarman *et al.* (14), as described in MATERIALS AND METHODS. Two kinds of fluorescent dyes were encapsulated, one that self-quenches when liposomes shrink (G, the green dye calcein, emitting at 519 nm) and the other that does not (R, the red dye sulforhodamine-101, emitting at 619 nm). Therefore, the G/R ratio reflects the osmolarity of the surrounding fluid. The lipid composition of the liposomes described by Jayarman *et al.* was not well defined, and the liposome response curves were non-linear (14). We tested different combinations of diacyl glycerophospholipids and their polyethylene glycol-modified derivatives. Liposomes made from mixtures of *E. coli* L-α-phosphatidylethanolamine, 1,2-dioleoyl-sn-glycero-3-phosphoethanolamine-*N*-[methoxy(polyethylene glycol)-2000], 1,2-dipalmitoyl-sn-glycero-3-phosphoethanolamine-*N*-[methoxy(polyethylene glycol)-5000], and cholesterol worked well at 30°C. They responded to the change in osmolarity linearly over a range of about 250 mOsm, as shown in Fig. 1C. We prepared the liposomes at 245 mOsm, so they could be used to measure up to 500 mOsm. These liposomes were stable up to a week when stored in argon at 4°C and up to 5 h when applied to a swarm plate in air at 30°C.

Since we used photon counting, the intensity of the excitation light was low, and the effect of photobleaching was small (Fig. 1A). Photobleaching was estimated by fitting the G/R ratio recorded in liquid suspension by linear regression. The data for the first 250 s were excluded to allow time for equilibration. The averaged slope of the fitting curves was $(3.75 \pm 0.7) \times 10^{-6}$ per second (mean ± SD, n = 9). This amount of photobleaching leads to a small correction

212 on all measured curves. The G/R ratios recorded between 300 s and 350 s were averaged for
213 plotting the standard curves in suspension (Fig. 1C); within this short time photo-bleaching was
214 small enough to be ignored.

215 To obtain the calibration curves on plates, the G/R values were corrected for photo-
216 bleaching and then extrapolated to the time of dispensing, so that evaporation through our
217 temperature-control apparatus could be ignored (Fig. 1B). The calibration curve thus generated
218 had a steeper slope than that found for liposomes in suspension (Fig. 1 D). The two curves
219 crossed at the point where the osmolarity of the agar matched that of the medium in which the
220 liposomes were prepared. The liposomes form a multilayer disk on the agar surface. It is likely
221 that if the agar surface and the liposomes are isotonic, the liposomes remain spherical and the
222 inter-liposome space is similar to that in suspension; while on an agar surface that is hypertonic,
223 the shrunken liposomes are more densely packed, like flattened balls. If so, the loss of light by
224 absorption or diffraction might be more severe in the green than in the red, leading to a decrease
225 in the G/R ratio. Whatever the reason, liposome packing caused a reduction of signal equal to
226 6.42 mOsm per 0.01 G/R ratio. The calibration curves for the scanning experiments were
227 obtained with liposome pads made from larger aliquots of liposomes equilibrated for shorter
228 periods of time, before dense packing became significant, so these curves were similar to those
229 obtained with liposomes in suspension.

230 **Monitoring osmolarity in swarms**

231 We first tried to monitor the change in osmolarity in real time, by collecting fluorescence signals
232 from a fully illuminated fixed liposome spot ~450 μm in diameter, as an advancing swarm ran
233 over it (Fig. 2). Although we used the same swarm medium to prepare the plates and the

liposomes, the medium in the liposome suspension needed more than 1 h to equilibrate with the medium in the agar. After equilibrating >1.5 h, traces of G/R ratios showed a quick decrease upon the arrival of bacteria, followed by slow recovery to a level slightly higher than the baseline before the invasion (Fig. 2B, with the long-time end of the trace not shown). In cases when swarms expanded rapidly, traces recorded after waiting for >1.0 h were occasionally used to calculate the changes in osmolarity.

At the beginning of each trace, there was a section where the fluorescence signals were recorded before the arrival of the swarm (Fig. 2). These signals provided a baseline for subsequent changes in osmolarity. The calibration curve measured on plates (Fig. 1D, black open diamonds) was applied. Extrapolating the baseline to the time when the liposomes were dispensed allowed us to estimate the osmolarity that supports active swarming under our experimental conditions (~296.8 - 316.2 mOsm). By changing the concentrations of NaCl and Eiken agar, we could obtain swarms that expanded at velocities ranging from 1.0 μm/s to 4.3 μm/s (Fig. S1 in the Supporting Material). There was an inverse correlation between swarming speed and agar osmolarity.

There was a transient increase of both the green and red signals when the swarm invaded the liposome spot (Fig. 2A). The swarm drew water out of the agar and lifted the liposomes from the packed state to the suspended state: the motionless liposomes began jiggling around when the bacteria arrived. This process suddenly increased the inter-liposome space, decreasing the loss of light by absorption or diffraction. Thereafter, a small amount of liposomes were carried away by the swarm fluid, causing a slow decrease of both fluorescence signals, but this process would not change the G/R ratio. It is the decrease of green fluorescence caused by self-quenching that is responsible for the persistent change of the G/R ratio (Fig. 2B).

After bacterial invasion, the calibration curve measured on agar is only applicable to some liposomes within the excitation field, while the curve in suspension would be applicable to the others. The measurements were corrected for the fraction of liposomes in the packed state vs. those in suspension, and the *bona fide* osmolarity was plotted in Fig. 2C. The distance inside the swarm (negative towards the swarm center) was determined by multiplying the time after invasion by the instantaneous velocity of the swarm front. The location of the leading edge of the swarms was at position 0.

Before the large increase of osmolarity shown in Fig. 2C, a small peak of width 51.0 ± 18.3 μm (n=6) always appeared (Fig. 2D, grey arrows). It was followed by a brief, sharp biphasic dip with recovery. We believe this peak was due to the arrival of the stream of fluid that flows in a clockwise sense in front of the swarm (12); see Fig. S2A. This small amount of fluid caused an increase of osmolariy 2.8 ± 0.9 mOsm. Within ~10 s the bacteria arrived, and a large amount of fluid flooded the spot.

The actively-expanding rim of a swarm can be divided into four regions (10, 11). The outermost region is a monolayer of cells, many of which are stuck on the agar surface. These cells are released when the cells of the second multilayer region, which are vigorously motile and at high density, catch up. The cell density decreases in the third region, dubbed the falloff, leading to the plateau, where motility remains at a relatively low level. When the monolayer cells (and some from groups in the high-density region) rushed onto the liposome spot (Fig. S2A), the cells dispersed into a band 130~150 μm wide, and the cell density decreased from ~0.18 cells/μm^2, as in the normal swarm monolayer, to ~0.03 cells/μm^2. This dispersed monolayer contained the same number of cells, but covered 4.5 times as large an area as the

279 monolayer on agar. The front edge of this dispersed monolayer was irregular in shape, with
280 dynamic protrusions and invaginations.

281 The osmolarity increased steadily upon the arrival of the cells, and then the rate of
282 increase slowed down, until an osmolarity maximum was reached (Fig. 2 D). The rapid increase
283 took about ~35s, while the slow increase that followed was swarm-speed dependent. The whole
284 process of this osmolarity jump took place within a distance slightly longer than the diameter of
285 the liposome spot, 480 ± 22 μm (n=6). The dispersed monolayer and multilayer regions moved
286 rapidly forward at 6.0 ± 1.0 μm/s (n= 5) until the dispersed monolayer reached the far edge of the
287 liposome spot. The osmolarity jump – the difference between the osmolarity maxima and the
288 baseline (Fig. 2C, double-headed arrow) – was 11.4 ± 5.0 mOsm (n=15). The steady level
289 reached at the end of the experiment was 3.7 ± 0.6 mOsm (n=15) higher than the baseline. This
290 value reflects the osmolarity of the swarm interior. When the monolayer cells reached the far
291 edge of the liposome spot, the cells stalled and the multilayer caught up with decreasing velocity
292 (Fig. S2A). Eventually, the swarm ran over the far edge of the liposome spot and continued
293 advancing on the agar. Because the swarm expanded faster on the liposome spot than on the
294 adjacent agar, a hump formed at the swarm front that eventually smoothed out.

295 **Scanning across swarms moving on liposome pads**

296 The fixed spots did not provide the spatial resolution required to evaluate the fluid-flow model
297 (10). Therefore, we performed another set of experiments in which the liposome pads were 5
298 times larger in diameter (Fig. 3). The excitation beam, 20 μm in diameter (not shown), was held
299 fixed, while the plate was pushed by a picomotor, so that the swarm was scanned in its direction
300 of motion, as shown by the small arrows in Fig. 3. The fast expansion rate of the swarm on the

liposome pad made the swarm spread out, so that the monolayer and multilayer regions of the swarms were cleanly separated from their counterparts on the agar surface (Fig. 3). Because the front of the dispersed monolayer was not uniform, we used the position of the monolayer/multilayer interface as our reference point (position 0).

To convert measurement time to distance, the speed of the excitation beam relative to the reference origin is required. To a first approximation, this is just the swarm speed less the plate pushing speed. For a second scan performed on the same plate, the swarm speed decreased as the dispersed monolayer approached the far end of the pad, so we linearly interpolated the swarm speed from 6 μm/s to the respective swarm expansion rate on agar. The resulting osmolarity vs. distance plots are shown in Fig. 4A.

The scanning experiment revealed that the multilayer region of the swarm contains two distinct bands, an outer high-osmolarity band of 327.1 ± 6.5 mOsm, and an inner low-osmolarity band of 302.5±5.0 mOsm (Fig. 4A). The osmolarity baseline on the agar surface measured with the fixed liposome spot under identical conditions was 302.1 ± 2.3 mOsm (n=8) (Fig 4A, dark and light orange lines). The outer band is therefore 25.3 ± 7.3 mOsm higher than the baseline and the inner band is almost isotonic to the agar. Farther inside there is a stable plateau that is 11.3 ± 3.1 mOsm higher than the baseline. The osmolarity eventually went down to the interior level that was 3.7±2.9 mOsm above the baseline. The dispersed monolayer, a band ~150 μm wide to the right of position 0, had an osmolarity 9.2 ± 5.3 mOsm above the baseline.

The osmolarity profile inside a bacterial swarm

The liposomes were covered with polyethylene glycol to increase stability, which has certain surface properties (e.g., hydrophilicity) that make swarms expand faster on liposome spots or

323 pads than on virgin agar. In the scanning experiments, different regions of the swarm were fully
324 expanded and well separated from their counterparts on agar (Fig. 3), but on the fixed spot, such
325 expansion was restricted (Fig. S2B). As a result, we did not see the low-osmolarity band on
326 spots: the low-osmolarity band is obvious in Fig. 4A but not in Fig 2D. Part of the problem was
327 the low spatial resolution of the fixed-spot method; for example, if the leading edge of a swarm
328 advances 50 μm over a spot of diameter 450 μm, the swarm will cover only 6% of the area of the
329 spot, and 94% of the light reaching the detectors will come from the cell-free region.

330 The fixed-spot measurements generated an osmolarity increment of 2.8 mOsm when the
331 fluid that flows in front of the swarms drained into the liposome spots. This is an underestimate
332 because, as noted above, most liposomes in the spots were not influenced by this small amount
333 of fluid. The experimental value was corrected by multiplying by the ratio of the area of the
334 whole spot to the area of the segment that was wetted by the flow. The height of this segment
335 was obtained by assuming that the width of the flow on agar was expanded 4.5 times. The
336 corrected osmolarity was as high as the plateau (12.1 mOsm), as shown in Fig 4B.

337 To find the dimensions of swarms on agar from the dimensions on liposome pads (Fig. 3),
338 we multiplied the dimensions on pads by 2.6/6.0, the ratio of the speeds on agar, 2.6 ± 1.0 μm/s
339 (n=15), to those on pads, 6.0 ±1.0 μm/s (n=5). The monolayer thus converted spanned 66 μm.
340 The width of the monolayer in a normal swarm measures 31 μm, on average (10). To compare
341 with the previous results, we used this smaller width and set the front of the monolayer as the
342 reference origin (Fig. 4B). The osmolarity of the monolayer was scaled using the dilution factor
343 of 4.5 mentioned above. This assumes that the fluid and the cells were diluted to the same
344 degree, which would be the case if the film of fluid expanded to its original thickness. We note

345 that the cells at the outer edge of the monolayer were transiently stuck to the agar, while those in
346 the multilayer were actively swimming (10, 11). The expanded multilayer on pads was filled by
347 cells that flowed in from the sides and thus maintained its thickness.

348 Mapping the fluid-flow pattern inside swarms with micron-sized air bubbles (10)
349 revealed that swarm fluid flows inwards from the edge of the swarm toward the center, while
350 beginning from ~300 μm inside the swarm, it flows outwards. Fluid balance requires that water
351 moves out of the agar and into the swarm within a region centered ~30 μm from the edge of the
352 swarm, with a peak at the monolayer/multilayer interface. After correcting for differences in
353 migration rates on pads vs. those on virgin agar, the osmolarity profile agreed well with the
354 model prediction (Fig. 4B). The osmolarity increased rapidly at the monolayer/multilayer
355 interface and reached the highest value at ~30 μm inside the swarm. The osmolarity profile for
356 the first ~130 μm paralleled the surface cell-density measured earlier (Fig. 5 of ref. 10).

357 Fluid balance also required that the agar absorb water from the swarm in a region
358 centered ~120 μm from the edge of the swarm. The lowest point on our curve was at -128 μm,
359 and it reached the baseline or slightly lower, within the error range of our measurements (Fig. 4A,
360 light orange dotted line). The osmolarity reached a stable plateau at ~200 μm from the edge of
361 the swarm (Fig. 4B), also in accordance with the model prediction (10). The maxima obtained in
362 the fixed-spot measurements corresponded to the plateau detected by scanning. It was ~11.3
363 mOsm higher than the baseline as revealed by both methods. This plateau extended to ~300 μm
364 inside the swarm. The osmolarity began to decrease beyond that point and reached the level for
365 the swam interior ~500 μm from the edge of the swarm. Active fluid flow was not observed
366 beyond 300 μm from edge of the swarm (10), suggesting that this region of the swarm is in
367 equilibrium with the agar.

368 **Properties of osmolytes**

369 The primary osmolyte that has been implicated in the swarming of *E. coli* or *Salmonella* is
370 lipopolysaccharide (17, 18). Other candidates of high molecular weight include enterobacterial
371 common antigen and colanic acid (18). Mutants of *Salmonella* that rotate their flagella
372 exclusively clockwise or exclusively counterclockwise fail to swarm, yielding plates that are
373 relatively dry (19). However, revertants that remain nonchemotactic yet frequently switch the
374 direction of flagellar rotation do swarm, leading to the suggestion that erratically-moving flagella
375 strip lipopolysaccharide off of the cell surface (20).

376 We need osmolytes of relatively high molecular weight (with relatively small diffusion
377 coefficients) to explain our results. Substances of low molecular weight, like salts, acetate,
378 glutamate, proline, glycine betaine, or trehalose, will not do. The swarm fluid is only a few μm
379 thick, while the underlying agar is ~1,400 μm deep. Both are nearly 100% water. A small
380 molecule with diffusion coefficient, D ~10^3 $\mu m^2/s$ (10^{-5} cm^2/s) will diffuse $(2Dt)^{1/2}$ ~2 μm in
381 ~0.002 s, 20 μm in ~0.2 s, and 200 μm in ~20 s. The time scale of interest (Fig. 4B) is about 50 s
382 (a swarm displaced ~130 μm at the rate of 2.6 μm/s). In that interval, substances of low
383 molecular weight will be diluted by a factor of more than 100 by diffusion perpendicular to the
384 surface of the plate, and peaks and troughs, such as those apparent in Fig. 4B, will be washed out
385 by diffusion in a direction parallel to the surface of the plate. But substances 100 times larger
386 with diffusion coefficients 100 times smaller will fit the bill. A substance of this size can diffuse
387 out of the swarm fluid into the agar (neglecting opposing fluid flow) in about 0.2 s, or into the
388 agar a distance 10 times as far, in about 20 s. So once the bulk flow subsides, the osmolyte will
389 move into the agar. Thus, one expects a concentration inversion when the measured value of the
390 osmotic pressure falls to the baseline, as it does in Fig. 4B. When this happens, some fluid will

391 flow from the swarm back into the agar. So the general features of our osmolarity measurements
392 are consistent with the predictions of the fluid-flow model. If the osmolytes are polyelectrolytic,
393 counter-ions will contribute to the osmolarily. We do not know whether the fall in concentration
394 of osmolytes is precipitated simply by a decreased rate of cell growth (10) or whether the
395 osmolytes are actively resorbed.

396 If the swarm spreads at 2.6 um/s, the peak in osmolarity shown in Fig. 4B extending from
397 0 to 520 um can be scanned in 200 s. We let the concentration of osmolyte at the surface of the
398 agar vary in time according to the output of this scan and follow the concentration of the secreted
399 osmolyte as it diffuses into the agar. We ask, as a function of the value of the diffusion
400 coefficient, D, how long it takes before the gradient normal to the surface of the agar changes
401 sign. This time interval would equal that measured earlier (10) before fluid begins to flow from
402 the swarm back into the agar, 41 ± 7 s. The acceptable range of diffusion coefficients proves to
403 be 0.7 to 6.8 $\mu m^2/s$, which is in the ballpark predicted by our order of magnitude arguments. A
404 diffusion coefficient in this range (1.1 $\mu m^2/s$) has been measured for aggregates of phenol-
405 extracted lipopolysaccharide of molecular weight ~$2x10^8$ (21). So lipopolysaccharide is an
406 attractive candidate.

407 Conclusion

408 We optimized the liposome sensor and used it to monitor the osmolality of bacterial swarms in
409 real time. The result revealed a well-defined osmolality profile inside the bacterial swarm. The
410 flow pattern of *E. coli* swarm fluid previously described was explained. The diffusion
411 coefficient of the potential osmolyte(s) was predicted based on our model. The chemical
412 structure of the osmolyte(s) remains a question for future investigation; although,

413 lipopolysaccharide is a reasonable candidate. This technique is highly reproducible when
414 applied to *E. coli,* which does not produce surfactants. The method can be applied to surfactant-
415 producing bacteria as well, provided that the surfactants are not strong enough to destroy the
416 liposomes. We look forward to the application of this technique in other swarming bacteria and
417 in other research fields.

418 ## Acknowledgments

419 This research was supported by NIH Grant AI100902. Author contributions: LP, YW, JT, and
420 HB designed the research; HB assembled the microscope; YW did preliminary work on the
421 liposome prep; YW and GH did preliminary work on the fluorescence measurements; GH
422 perfected the data-acquisition system; JT helped with the scanning experiments; LP did the final
423 measurements and analyzed the data; LP and HB wrote the paper, with input from the other
424 authors. The authors declare no conflict of interest.

425

REFERENCES

1. Harshey, R. M. 2003. Bacerial motility on a surface: Many ways to a common goal. Annu. Rev. Microbiol. 57:249-273.
2. Kearns, D. B. 2010. A field guide to bacterial swarming motility. Nat. Rev. Microbiol. 8:634-644.
3. Berg, H. C. 2005. Swarming motility: It better be wet. Curr. Biol. 15:R599-R600.
4. Hola, V., T. Peroutkova, and F. Ruzicka. 2012. Virulence factors in *Proteus* bacteria from biofilm communities of catheter-associated urinary tract infections. FEMS Immunol. Med. Microbiol. 65:343-349.
5. Callegan, M. C., B. D. Novosad, R. Ramirez, E. Ghelardi, and S. Senesi. 2006. Role of swarming migration in the pathogenesis of *Bacillus* endophthalmitis. Invest. Ophthalmol. Vis. Sci. 47:4461-4467.
6. Murray, T. S., M. Ledizet, and B. I. Kazmierczak. 2010. Swarming motility, secretion of type 3 effectors and biofilm formation phenotypes exhibited within a large cohort of *Pseudomonas aeruginosa* clinical isolates. J. Med. Microbiol. 59:511-520.
7. Medina-Ruiz, L., S. Campoy, C. Latasa, P. Cardenas, J. C. Alonso, and J. Barbé. 2010. Overexpression of the *recA* gene decreases oral but not intraperitoneal fitness of *Salmonella enterica*. Infect. Immun. 78:3217-3225.
8. Harshey, R. M., and T. Matsuyama. 1994. Dimorphic transition in *Escherichia coli* and *Salmonella typhimurium*: surface-induced differentiation into hyperflagellate swarmer cells. Proc. Natl. Acad. Sci. U.S.A. 91:8631-8635.
9. Berg, H. C. 2004. *E. coli* in Motion. Springer-Verlag Inc., New York.
10. Wu, Y., and H. C. Berg. 2012. Water reservoir maintained by cell growth fuels the spreading of a bacterial swarm. Proc. Natl. Acad. Sci. U.S.A. 109:4128-4133.
11. Darnton, N. C., L. Turner, S. Rojevsky, and H. C. Berg. 2010. Dynamics of bacterial swarming. Biophys. J. 98:2082-2090.
12. Wu, Y., B. G. Hosu, and H. C. Berg. 2011. Microbubbles reveal chiral fluid flows in bacterial swarms. Proc. Natl. Acad. Sci. U.S.A. 108:4147-4151.
13. Turner, L., R. Zhang, N. C. Darnton, and H. C. Berg. 2010. Visualization of flagella during bacterial swarming. J. Bacteriol. 192:3259-3267.
14. Jayaraman, S., Y. Song, and A. S. Verkman. 2001. Airway surface liquid osmolality measured using fluorophore-encapsulated liposomes. J. Gen. Physiol. 117:423-430.
15. Armstrong, J. B., J. Adler, and M. M. Dahl. 1967. Nonchemotactic mutants of *Escherichia coli*. J. Bacteriol. 93:390–398.
16. Turner, L., A. S. Stern, and H. C. Berg. 2012. Growth of flagellar filaments of *Escherichia coli* is independent of filament length. J. Bacteriol. 194:2437-2442.
17. Toguchi, A., M. Siano, M. Burkart, and R. M. Harshey. 2000. Genetics of swarming motility in *Salmonella enterica* Serovar Typhimurium: Critical role for lipopolysaccharide. J. Bacteriol. 182:6308-6321.
18. Partridge, J. D., and R. M. Harshey. 2013. Swarming: Flexible roaming plans. J. Bacteriol. 195:909-918.
19. Wang, Q., A. Suzuki, S. Mariconda, S. Porwollik, and R. M. Harshey. 2005. Sensing wetness: a new role for the bacterial flagellum. EMBO J. 24:2034-2042.
20. Mariconda, S., Q. Wang, and R. M. Harshey. 2006. A mechanical role for the chemotaxis system in swarming motility. Mol. Microbiol. 60:1590-1602.

471 21. Hartley, J. L., G. A. Adams, and T. G. Tornabene. 1974. Chemical and physical
472 properties of lipopolysaccharide of *Yersinia pestis*. J. Bacteriol. 118:848-854.

473

FIGURE LEGENDS

Fig. 1. Calibration of osmolarity-sensitive liposomes. **A**, the G/R fluorescence ratio recorded over an interval of 500 s when liposomes prepared at 245 mOsm were suspended in swarm media at the osmolarities indicated on the plot. Note the minimal effect of fluorescence bleaching on the G/R ratio. **B**, G/R ratios from liposomes that were loaded on agar surfaces 0.5 h before recording. Osmolarities of the swarm media used to prepare the plates were measured after the media and agar were separated by centrifugation. These values are shown on the plot. The dotted lines show the data after correction for photo-bleaching. The changes that remain are due to evaporation. **C**, G/R ratios at medium osmolarities recorded between 300 and 350 s. **D**, Comparison of the G/R ratios measured in suspension (red circles) to those measured on an agar surface (black diamonds) as a function of the osmolarity of the swarm media.

Fig. 2. Change of osmolarity on swarm plates measured with fixed liposome spots. **A**, The fluorescence signals of sulforhodamine 101 (R) and calcein (G) recorded on a swarm. Time zero corresponds to the time when bacteria first invaded the liposome spot. **B**, The G/R ratio after correction for photo-bleaching. The grey dotted line is the reference baseline for osmolarity on the agar surface, which changed because of evaporation. The time required for the measurement, set by the dimensions of the swarm divided by its spreading rate, was relatively long. **C**, The trace after the G/R ratio was converted to osmolarity and time was converted to distance (negative toward the swarm center). The grey dotted line is the reference baseline. It curved down because the evaporation rate was constant, but the swarming speed slowed down. The initial swarming speed was 1.0 μm/s. The grey broken line indicates the osmolarity maximum, and the double-headed arrow the difference in osmolarity between the maximum and the baseline. The difference between the osmolarity trace and the baseline was maximum between

497 the two grey down-pointing arrows. **D**, An enlarged view of the boxed region in **C** with two
498 other traces aligned on top of it (with swarm speeds in μm/s noted at the right ends of the traces).
499 The small peak at time zero is indicated by grey arrows. The osmolarity maxima are highlighted
500 by grey bars superimposed on the traces.

501 **Fig. 3.** A diagram showing a swarm that has arrived at the center of a liposome pad, 2.3 mm in
502 diameter. Different grey-scale values represent different swarm regions, as labeled in the figure.
503 The black dotted line indicates the swarm front. Arrows show the direction of the scan.

504 **Fig. 4.** Change of osmolarity inside swarms spreading on liposome pads revealed by scanning.
505 Position 0 corresponds to the monolayer/multilayer interface. Negative values are toward the
506 center of the swarms. **A**, Means (black line) and standard deviations (grey areas) from 9 scans
507 on 7 different plates. The osmolarity baseline measured on the agar surface is shown by a dark
508 orange line, and its standard deviation by light orange dotted lines. Note that each scan was
509 completed in less than 2 min with liposomes submerged in swarm fluid, so evaporation was not a
510 problem. **B,** The osmolarity profile inside a swarm after subtraction of the baseline value for
511 virgin agar and conversion of the distance on the liposome pad to that on agar. The grey open
512 circles are measured values and the black line is the curve that fits the data. The monolayer was
513 normalized (shrunk to normal size) and the reference point was set to the front. The osmolarity
514 values were corrected for dilution that occurred when the swarms spread over the liposome pads.
515 The notations monolayer, multilayer, falloff, and plateau refer to regions of different surface cell-
516 density described in ref. 11.

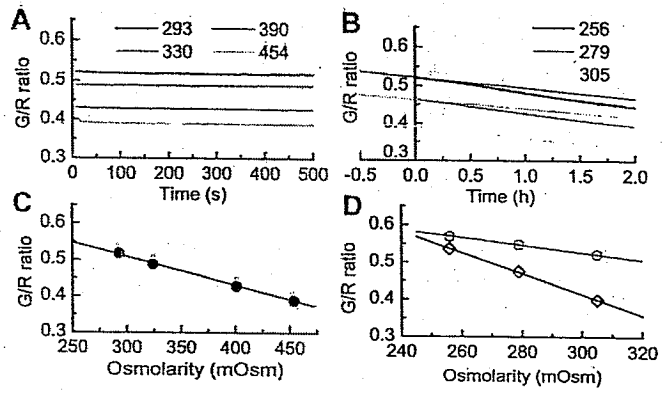
A
293
390
330
454
G/R ratio
0.6
0.5
0.4
0.3
0
100
200
300
400
500
Time (s)
B
256
279
305
G/R ratio
0.6
0.5
0.4
0.3
-0.5
0.0
0.5
1.0
1.5
2.0
Time (h)
C
G/R ratio
0.6
0.5
0.4
0.3
250
300
350
400
450
Osmolarity (mOsm)
D
G/R ratio
0.6
0.5
0.4
0.3
240
260
280
300
320
Osmolarity (mOsm)

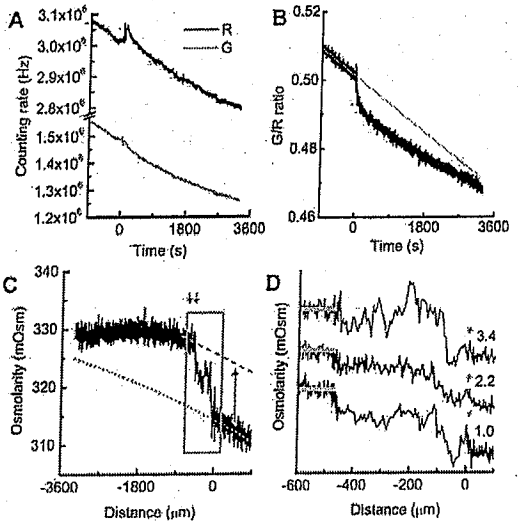

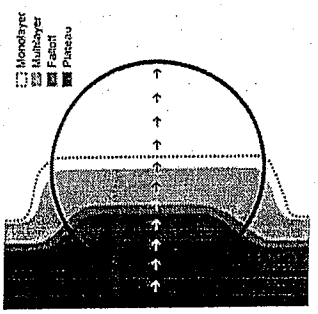
Monolayer
Multilayer
Facet
Plateau

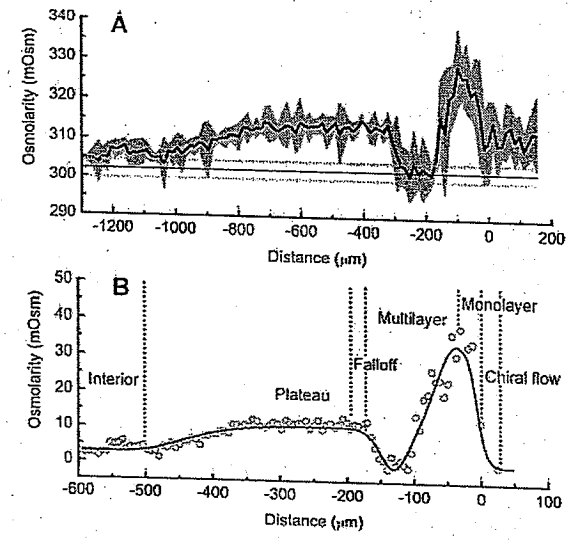
A
Osmolarity (mOsm)
340
330
320
310
300
290
-1200
-1000
-800
-600
-400
-200
0
200
Distance (μm)
B
Osmolarity (mOsm)
50
40
30
20
10
0
Interior
Plateau
Falloff
Multilayer
Monolayer
Chiral flow
-600
-500
-400
-300
-200
-100
0
100
Distance (μm)

The NIHMS has received the file 'mmc1.pdf' as supplementary data. The file will not appear in this PDF Receipt, but it will be linked to the web version of your manuscript.

Supporting Material

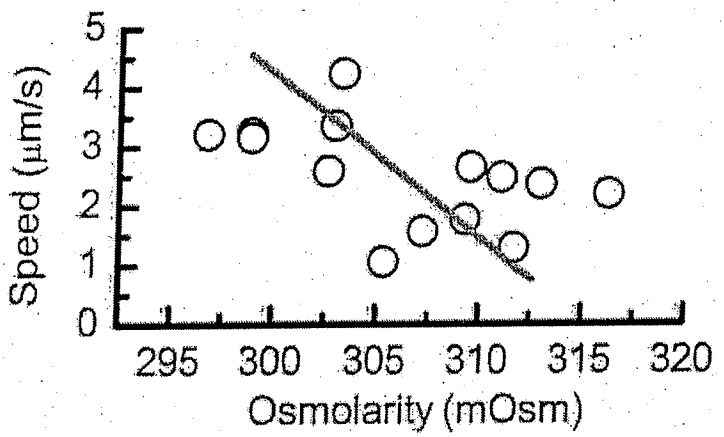

Fig. S1. Dependence of initial swarm speed on agar osmolarity, with a linear fit.

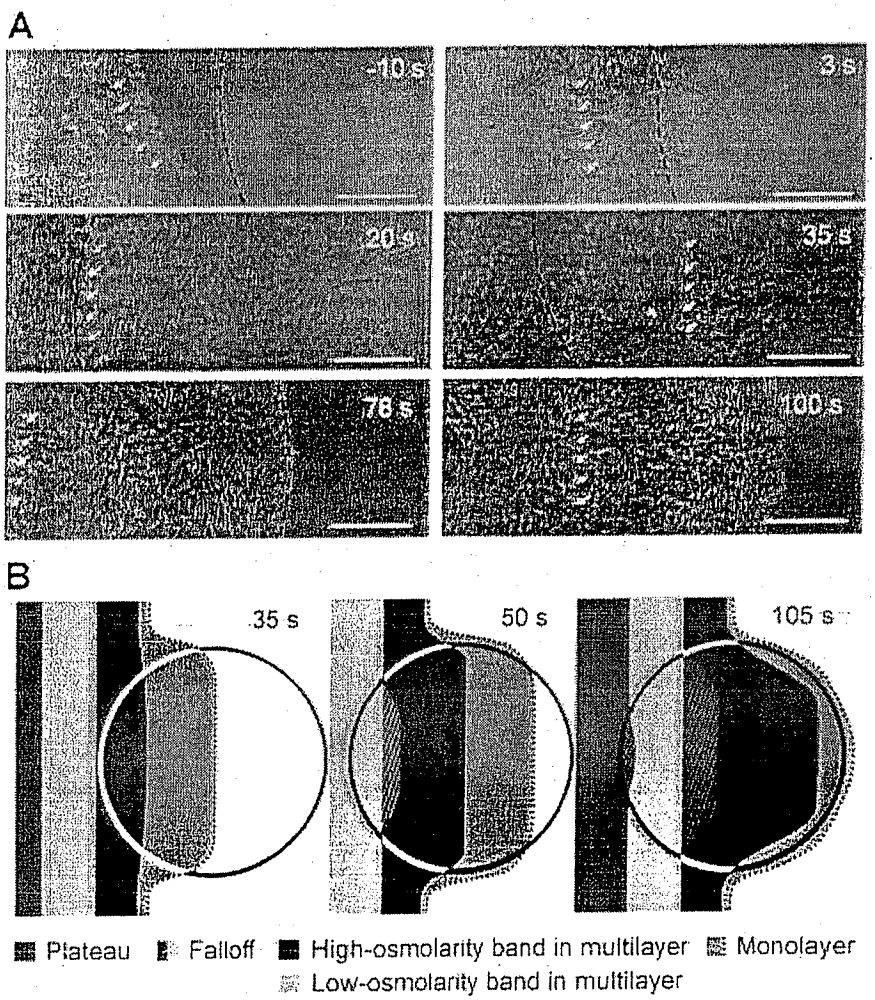

Fig. S2. Interaction between bacteria and a fixed liposome spot. **A**, Snapshots of swarms running over liposome spots taken from three different movie clips. Broken arches depict the proximal or distal edges of the liposome spots. The chiral flow in front of the swarm appears as slightly dark shade. Scale bars equal 50 μm. Approximate times relative to the initial time of invasion are shown on the top-right corner. White arrows highlight the monolayer/multilayer interfaces. **B.** Diagrams showing the movement of a swarm on liposome spots at different times. Grey levels correspond to cell densities and osmolarities of different regions of the swarm, as indicated in the bottom legend. The black dotted line is the swarm front. Shading indicates the minimal area where cells from swarm regions might have mixed.